Hierarchy of abrupt transitions in the past climate

Denis-Didier Rousseau, Valerio Lucarini, Witold Bagniewski

Science Advances
AAAS

Manuscript Template

FRONT MATTER

Title

- Full title: The hierarchy of abrupt transitions that shaped the past climate
- Short title: Cenozoic climate domino effect.

Authors

Denis-Didier Rousseau[1,2,3 *], Valerio Lucarini[4,5], Witold Bagniewski[6]

Affiliations

[1] Université Montpellier, Géosciences Montpellier, Montpellier, France
[2] Silesian University of Technology, Institute of Physics-CSE, Division of Geochronology and Environmental Isotopes, Gliwice, Poland
[3] Columbia University, Lamont Doherty Earth Observatory, New York, USA
[4] University of Reading, Department of Mathematics and Statistics, Reading,
[5] University of Reading, Centre for the Mathematics of Planet Earth, Reading, UK
[6] Ecole Normale Supérieure – Paris Sciences et Lettres, Laboratoire de Météorologie Dynamique, Paris, France

(*) corresponding author: denis-didier.rousseau@umontpellier.fr.

Abstract

The Earth's climate has experienced numerous critical transitions during its history. Such transitions are evidenced in high-resolution records covering different timescales. This suggests the possibility of identifying, ranking past critical transitions, which yields a more complex perspective on climatic history. Such a context allows defining dynamical climate landscapes with multi-scale features. To illustrate such a richer structure, we have analyzed 2 key high-resolution datasets: the CENOGRID marine compilation (past 66 Myr), and North Atlantic U1308 record (past 3.3 Myr). Our aim was to examine objectively the observed visual evidence of abrupt transitions and to identify among them, the key thresholds indicating regime changes that differentiate among major clusters of variability. This identification is discussed after comparison with major climate factors. A hierarchy in the observed thresholds is proposed through a domino-like succession of abrupt transitions, corresponding to as many bifurcations that shaped the Earth's climate system over the past 66 Ma.

Teaser

A hierarchy of Tipping Points shaped the Earth past climate following domino-like effects implying a future major bifurcation in the climate system.

MAIN TEXT (The manuscript should be a maximum of 15,000 words)

Introduction

Early evidence of abrupt transitions in Camp Century and Dye 3 Greenland ice cores (*1*, *2*) attracted a lot of attention from the paleoclimatic community before being well acknowledged and understood. They have indeed introduced the evidence of a chain of abrupt climatic variations that at the time were unknown. Nonetheless, such transitions did not seem to find an agreement with other marine and terrestrial records, which led to considerable debate in the field (*3–5*). After decades spent retrieving and studying much more detailed paleorecords, the evidence for such rapid climatic variations, named Dansgaard-Oeschger events (DO), has been well accepted since then. They have been recently reinforced by the identification of additional abrupt transitions from the NGRIP ice core, which have been made possible by the increased time-resolution of the record (*6*). These additional events correspond to changes of either short duration or amplitude in $\delta^{18}O$ that visual inspection of or standard statistical inspections do not necessarily flag. Moreover, such new series of abrupt transitions have been described from marine (*7*) and continental (*8*) records, among other, providing a broader spatial perspective to that specific dynamical process for the climate system. Although interpreted as to be related to the last climate cycle, these abrupt transitions occurring in the last 130 Kyr, have also been described in older records (*9–11*), recent studies implying that DOs are likely to have existed since 0.9 Ma (*12*) or even earlier (*13*).

The Earth climate has experienced numerous abrupt and critical transitions during its long history (*14*, *15*). Such transitions are evidenced in precise high-resolution records at different timescales. They have been interpreted as associated with abrupt climate changes, often corresponding to transitions, tipping points, leading to possibly irreversible changes in the state of the system. The study of tipping points has recently gained broad interest and perspective in Earth and Environmental sciences, especially with regard to the future of our societies under the present climate warming scenarios (*16–19*). The term Tipping Elements (TE) was introduced by (*18*, *20*), and subsequently adopted by others (*17*, *21*) to characterize the particular components of the Earth System that are likely to experience a tipping point (anticipated TPs) in a near future. These TEs relate to all the components of the Earth system: the atmosphere, the cryosphere, the ocean, the land surface and the biosphere, and are more or less interconnected (*19*, *22*, *23*). More recently tipping point concept starts being applied to socio-economical features (*24*, *25*).

To illustrate such an idea, we have analyzed 2 key high-resolution datasets of the past 66 Myr and showing evidences of abrupt transitions. The first time series is the CENOGRID benthic $\delta^{18}O$ and $\delta^{13}C$ corresponding to the compilation of 14 marine

records over the past 66 Myr (*26*). The second corresponds to the North Atlantic U1308 benthic $\delta^{18}O$, $\delta^{13}C$ and d^{18}bulk carbonate records covering the past 3.3 Myr (*27*). The aim was to examine the observed visual evidences of abrupt transitions and to identify among them key abrupt thresholds by applying the Kolmogorov-Smirnov (KS) test and the recurrence quantification analysis (RQA) (*28*),-see methods). In a second step, the selected transitions are discussed and replaced in the Earth climate history allowing the definition of dynamical succession of abrupt transitions. In a third step, we replace the potential succession of abrupt transitions in time series of key climate factors such as CO2 concentration, average global sea level, and depth of the carbonate compensation. The forth step searches for the presence of a nontrivial structure for the recurrence plot that would be indeed indicative of the multiscale nature of the quasi-potential of the benthic $\delta^{18}O$ and $\delta^{13}C$. This leads to conclude by proposing a potential hierarchy in the observed thresholds, and the definition of a domino-like succession of abrupt transitions that shaped the Earth climate system over the past 66 Ma.

Results

The KS augmented test of the benthic $\delta^{18}O$ record of the past 66 Ma identifies six major abrupt transitions corresponding to two major warming events at about 58Ma and 56Ma, followed by four major coolings at 47Ma, 34Ma, 14Ma and 2.9 Ma respectively (Fig. 1a). These events are classical ones described from the literature (*29*), where the first two transitions led to warmer conditions, while the latter four led to colder conditions. The recurrence plot (RP) and recurrence rate (RR) analyses of the same dataset identify also these major transitions, with a few more –like at 63Ma, 40Ma and 9.7Ma (Fig. 1c, Suppl. Tab. 1). We have chronologically labeled these TP1 to TP9. All these abrupt events are associated with clusters at different scales in the RPs, and, in particular are separated into two different macroclusters prior and after 34 Ma, the well-known Eocene-Oligocene Transition (EOT) (*30*). Such pattern characterizes two different types of variability regimes illustrating two types of state of the Earth Climate System (see Fig. 1b).

The older macrocluster shows a disrupted variability, according to Marvan nomenclature (*31*), bounded by the abrupt transitions identified at 66 Ma and 34 Ma respectively. Such

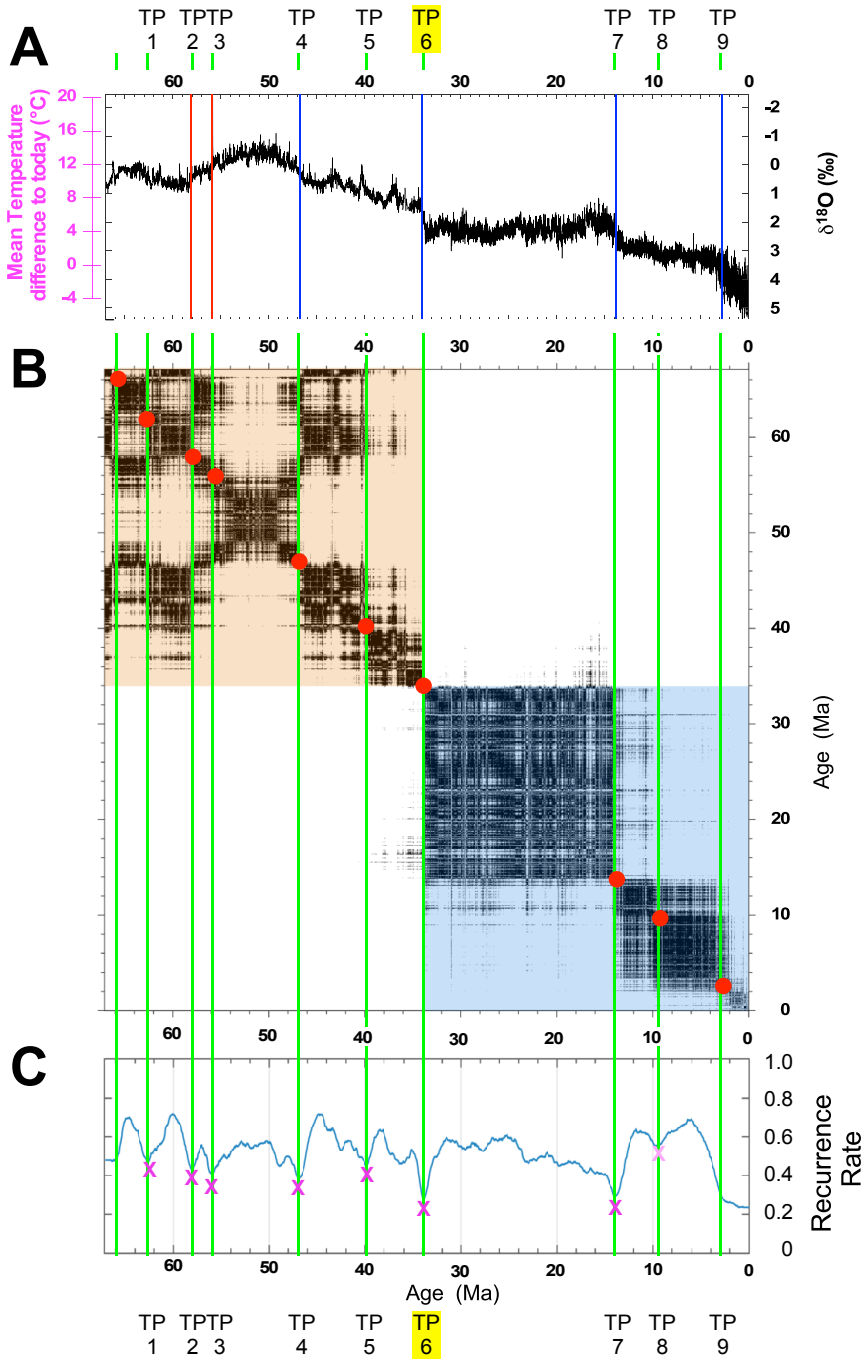

Fig. 1. **KS test and Recurrence Quantitative Analysis (RQA) of CENOGRID benthic $\delta^{18}O$.** A) Time series in Ma BP with difference of the reconstructed and present Mean Global Temperature in pink). KS test identifying abrupt transitions towards warmer conditions in red and cooler or colder conditions in blue; B) Recurrence plot (RP) with identification of the main two clusters prior and after 34 Ma. The main abrupt transitions identified are highlighted by red circles, and C) Recurrence rate (RR). The pink crosses and vertical green lines indicate the abrupt transitions (TP) detected by the RQA. CENOGRID benthic $d^{18}O$ data are from (*26*)

particular distribution corresponds to a response of the Earth system to some particular forcings to be determined later in the study. The main features of the oldest cluster are the most negative values of the benthic $\delta^{18}O$ corresponding to the very warm climate conditions that were prevailing between 66 Ma and 34 Ma. The average global temperature was estimated to be between 8°C and 16°C above the present day one (*26*) (Fig. 1a). No evidence of the presence of any major continental ice bodies is

recorded by the $\delta^{18}O$ values. However with this warm period further, hierarchically yet relevant abrupt transitions are found, including 2 major abrupt warmings at 58 Ma (TP2) and 56 Ma (TP3) respectively detected by both methods. These two transitions correspond to thresholds towards much warmer oceanic deep water corresponding to the first late Paleocene-Eocene hyperthermal (*32*, *33*) and Paleocene-Eocene Thermal Maximum (PETM) (*34*, *35*) respectively. The third one at about 47 Ma (TP4) corresponds to a transition towards cooler deep waters and named the Early-Middle Eocene cooling (*33*).

The more recent macrocluster presents, on the contrary, a different pattern indicating a repetition of sub-clusters showing a drifting variability from 34 Ma onward, characterizing non-stationary systems with slowly varying parameters. This second state characterizes colder climate conditions prevailing from 34 Ma to present day. This cold climate macrocluster is characterized by more positive values of benthic $\delta^{18}O$ and shows about 20 Myr of mostly stationary climate until 14 Myr (TP7) (*36*, *37*). Three abrupt transitions during the last 14 Myr, are associated, in the recurrence plot, to the presence of four recurrent patterns occurring at consecutive times: from 34 Ma (TP6) to 14 Ma (TP7), from 14 Ma to 9.7 Ma (TP8), from 9.7 Ma to 2.9 Ma (TP9), and from 2.9 Ma to present. These may be rather related to some internal factors of the Earth climate system, as described for more recent timescales (*12*, *28*).

Such general pattern of the RP for the 66 Myr translates an apparent irreversibility of the climate responses at 34 Ma (TP6), a date that must be therefore interpreted as a major threshold, a hierarchically dominant tipping point associated with the transition between two fundamentally different modes of operation of the climate system, represented by the two macro clusters.

Contrary to the benthic $\delta^{18}O$, the $\delta^{13}C$ RP shows a different pattern. Benthic $\delta^{13}C$ values rather characterize deep-water ventilation with high $\delta^{13}C$ values in regions close to deep-water formation area. The recurrence plot and recurrence rate analyses of the benthic $\delta^{13}C$ record yield 10 abrupt transitions among which three at 56.15 Ma, 34 Ma, and 7.15 Ma on the contrary respectively appear more important (SuppFig. 1, Suppl. Tab. 1). The interval 56.15 Ma – 7.15 Ma is well individualized showing some subclusters distributed around 34 Ma, which is identified, once more, as a key threshold. The 56.15 Ma date groups $\delta^{13}C$ values above 1‰, at the base of the record, while 7.15 Ma gathers the negative $\delta^{13}C$ values which mainly occurs on top of the record. These intervals are themselves characterized by two very different and opposed climate conditions with regards to a reference state represented by the 56.15 Ma – 7.15 Ma

interval. The upper climate regime translates more addition of carbon in the ocean while the lower cluster rather characterizes more addition of carbon in the atmosphere. These different thresholds are also identified by the KS test, which nevertheless detects some more at about 54.5 Ma, 37.5 Ma, and 16 Ma. A last threshold is identified with two different dates according to the method applied: 22 Ma from the KS test and 23 Ma from RP analysis.

The past 3.3 Ma record from North Atlantic core U1308, can be considered as a blow up of the CENOGRID dataset over this particular time interval (Fig. 2). The variations in the deep-water temperature, as expressed by the benthic $\delta^{18}O$, are also interpreted as an indicator of the continental ice volume with clear interglacial-glacial successions (*38–40*). The KS augmented test of the benthic $\delta^{18}O$ allows identifying the classical transitions characterizing the Marine Isotope Stages (MIS) as already observed in numerous records covering that interval (see (*12*) and herein). Such observation illustrates the clear response, during this interval, of the Earth Climate system to the classical external forcings (mostly obliquity at the base and eccentricity on top of the record) expressed in the astronomical theory of climate (*27, 41, 42*). The critical transition of the Mid-Pleistocene (MPT), between 1.25Ma and 0.8Ma, is well evidenced. The RP and RR of the benthic $\delta^{18}O$ record of U1308 indicate a drifting regime. This pattern appears similar to that already identified in the youngest macrocluster, for the recent 34Myr, determined also from the benthic $\delta^{18}O$ CENOGRID record. In U1308, it individualizes particular abrupt transitions responses at 2.93 Ma, 2.52 Ma, 1.51 Ma, 1.25 Ma, 0.61 Ma, and 0.35 Ma respectively (see Fig. 2b,c, Suppl. Tab. 1 - (*12*)). As they transition with the CENOGRID record, the abrupt thresholds at 2.93 Ma and 2.52 Ma have been labeled TP9 and TP10. On the contrary, the youngest transitions are interpreted as critical transitions and labeled CT1 (1.5 Ma) to CT4 (0.35 Ma) (Fig. 2)

Contrary to the CENOGRID $\delta^{13}C$ RP, U1308 $\delta^{13}C$ RP shows a drifting pattern similar to that of benthic $\delta^{18}O$, with only 2 key transitions at 2.52 Ma and 0.48 Ma (see Suppl. Fig. 3). However, beside the 2.52 Ma date, the 0.48 Ma does not have any equivalent in the benthic $\delta^{18}O$ records.

A complementary RQA of the $\delta^{18}O$ bulk carbonate record from U1308, which characterizes episodes of iceberg calving into the North Atlantic Ocean, and therefore illustrates the

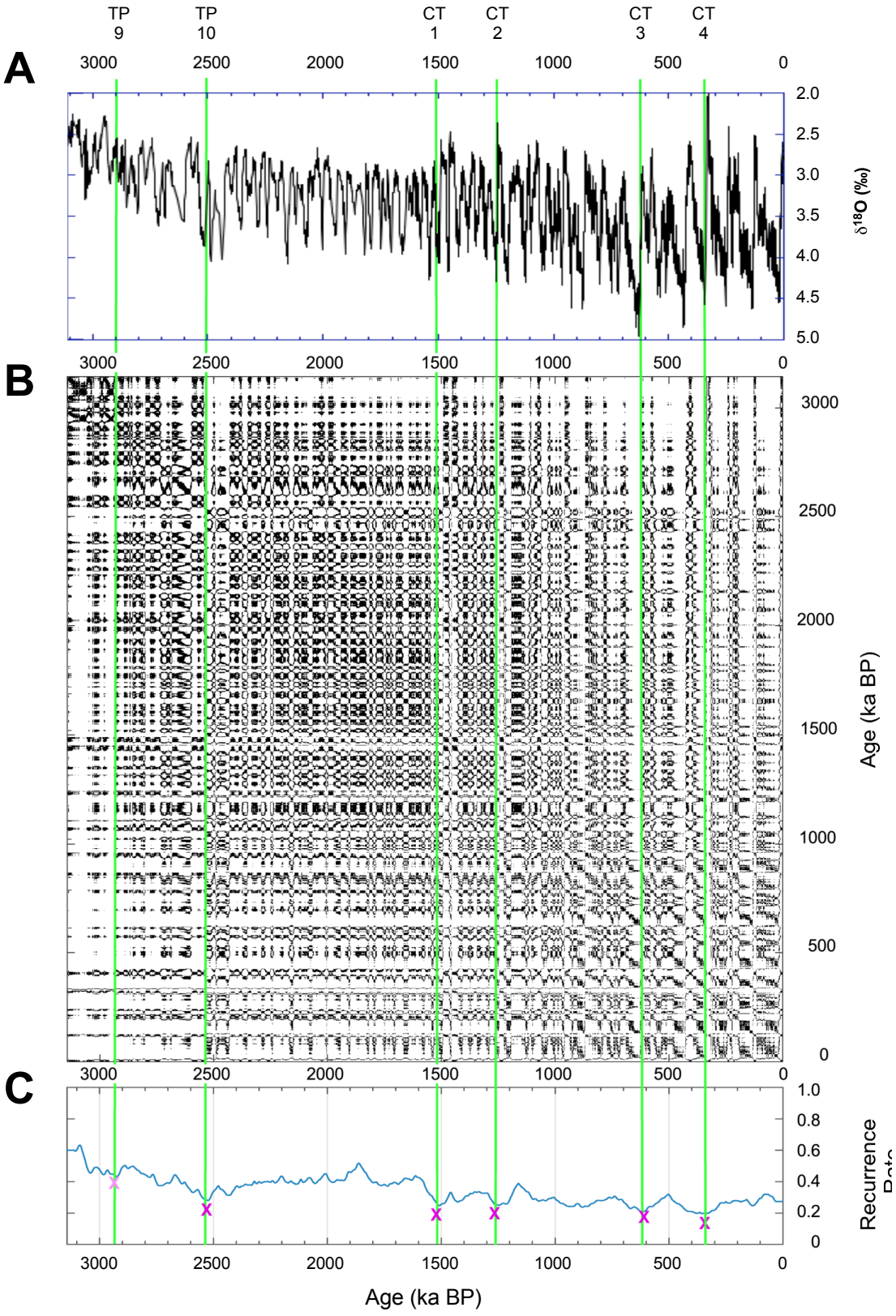

Fig. 2. **RQA of U1308 benthic $\delta^{18}O$.** A) Time series in Ma; B) RP; and C) RR. Crosses similar than Fig. S1. TP9-10 and CT1-4 abrupt transitions identified in the RR. U1308 benthic $\delta^{18}O$ data are from (*27*)

dynamics of the Northern Hemisphere ice sheets (NHIS), yields almost similar dates than those obtained for the benthic $\delta^{18}O$ record (see Suppl. Fig. 3, Suppl. Tab. 1) (*12*). Finally, when zooming over the last 0.7 Ma of U1308 benthic $\delta^{18}O$ record, the RP

shows a particular pattern of periodicity, with the last 0.65 Ma differentiated into 3 sub-clusters before the present interglacial (0.10 Ma), bounded respectively at 0.61 Ma, 0.43 Ma, 0.35 Ma and about 0.15 Ma.

Discussion

Replacing the different dates identified by the KS test and RQA from our two key records on a chronological perspective, the determined transitions appear in a particular order, with the threshold at 34Ma, corresponding to Eocene-Oligocene Transition (EOT), being central in the Cenozoic climate history. Indeed, after 66 Ma, the Earth is highly recovering from the intense reset provoked by the Chicxulub Meteorite impact (*43–46*) affecting both the Earth's climate and biodiversity as indicated through three different factors that are discussed below.

1 The Past 66Myr – 3 Myr history of the Earth Climate

Using benthic foram $\delta^{18}O$ and Mg/Ca records from high-resolution Pacific cores different from CENOGRID ones, (*33*) have reconstructed the variations of the global mean sea level (GMSL) of the past 66 Ma. GMSL has strongly impacted the global oceanic circulation, and determined the extent of the emerged and inundated land areas, especially the continental shelves allowing or preventing, associated to plate tectonics, continental biological migrations. Measuring the carbonate content in sediment Pacific cores and applying transfer functions, (*47*) have computed a detailed Cenozoic record of the Pacific carbonate compensation depth (CCD) below which carbonates dissolve. CCD represents therefore an indicator of the ocean carbonate saturation state and is linked to the atmospheric CO_2 concentration present above the sea surface. Finally, compiling estimates from various proxies including foram $\delta^{13}C$, boron isotopes, stomata, paleosols… (*48*) have released a comprehensive Cenozoic record of the CO_2 concentration that shows a large variability especially for the older interval, due to greater uncertainties in the reconstructions. We have thus replaced the major thresholds (TP) detected in our KS test and RQA against the GMSL, CCD, and CO_2 time series to interpret our results (Fig. 3).

One first notices that TP6 major transition at 34 Ma (EOT) is observed once more in the three factors, corresponding to an abrupt lowering of the GMSL of about 70m, of the CCD of around 1000m, of the CO_2 concentration, which are considerable changes (Fig. 3). TP6

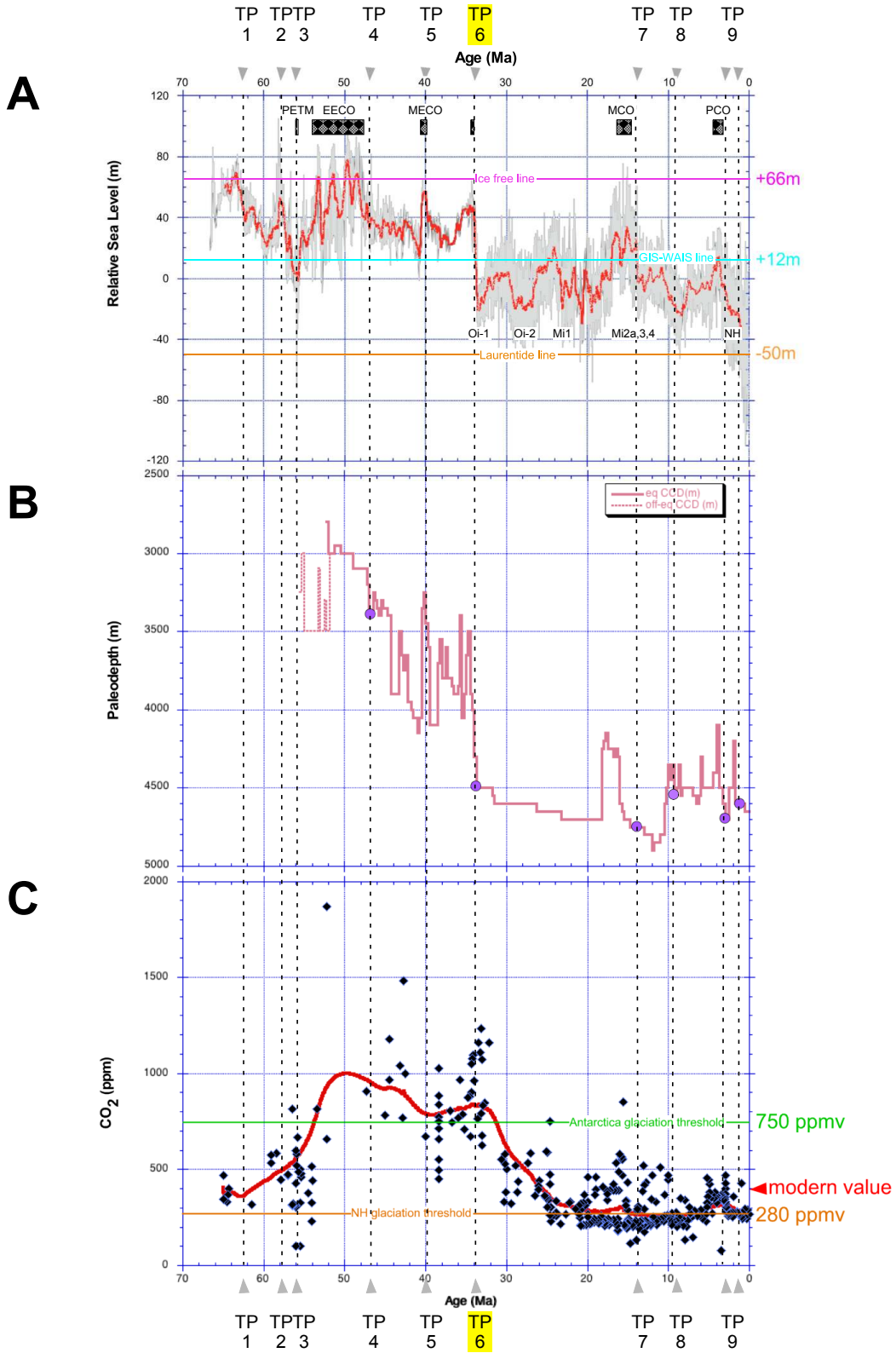

Fig. 3; **Variation through time of three main climate factors and comparison with the identified abrupt transitions (TP) in the CENOGRID benthic $\delta^{18}O$.** A) Global Mean Sea Level in meters from (*33*). Identification of particular warm and of glaciation events. The Laurentide, GIW-WAIS and Ice free lines are from (*33*); B) Carbonate Compensation Depth (CCD) in meters from (*47*). The purple circles identify the TPs on this record; C) Estimate of the CO_2 concentration in parts per million volume (ppmv) from (*48*). The Antarctica glaciation threshold at 750 ppmv and the NH glaciation threshold at 280 ppmv lines respectively are from (*85*)

splits these three time series into the same two main intervals than those previously observed from the RQA of the CENOGRID benthic $\delta^{18}O$ and $\delta^{13}C$ records. Such result

suggests therefore that correspondences may exist between these factors and the two parameters (Figs. 1,3, Suppl. Tab. 2), which differed prior and after EOT. An evident variability appears in the responses of the climate to various mechanisms, under four identified states, from ”Warmhouse” (66Ma-TP2 and TP4-TP6) and ”Hothouse” (TP2-TP4) climates, to ”Coolhouse” (TP6-TP7) and ”Icehouse” climates (TP7 to present); (see Fig. 1),

The first two states alternated, from 66 Ma until 34 Ma, in a warm-hot-warm sequence under extremely high CO_2 concentrations (*48*) compare to those measured over the past 800 Kyr in the Antarctic ice cores, which represent the reference states for the IPCC potential scenarios of climate change warming (*49*) (Fig. 3c). This first main interval shows the highest values of the Cenozoic era in GMSL, CO_2 concentration and CCD depth whose average values are: +38.47 ± 14.85m, 626.96 ± 311.79 ppmv and 4586 ± 153.01 m respectively (Suppl. Tab. 2). Conversely, the last two states succeeded each other, from 34 Ma onward present time, under much lower CO_2 concentrations and GMSL, thus generating the classical climate trend towards the recent ice-age conditions (*15*, *26*, *29*) (Fig. 3a,c). Indeed the last 34 Myr show average values in GMSL, CO_2 concentration and CCD depth of -3.49 ± 12.90 m, 329.89 ± 164.47 ppmv and 3518.67 ± 408.92 m respectively (Tab. 2), which are much lower than in the older interval. This second set of means are underestimated values because the final values of (*33*) dataset ending at 0.9Ma,

These GMSL, CCD and CO_2 reconstructions shows key transitions that fit with the CENOGRID thresholds deduced from the KS and RR analysis of the benthic $\delta^{18}O$ although they characterize either an increase or a decrease in the global mean sea level corresponding roughly to warming or cooling episodes of the Earth history or strong variations in the concentration of atmospheric CO_2. The variations observed in CO_2, CCD and GMSL, at the 10 identified TPs from the benthic $\delta^{18}O$ record, indicate inhomogeneous characteristics prior TP6 major threshold (Suppl. Tab. 3). On the contrary homogenous trends are noticed in the three climate proxies after TP6, translating the occurrence of major reorganizations in the climate system, which become interesting to test at a shorter timescale.

Studying the same CENOGRID dataset, (*50*) identified 9 geological transitions at respectively 62.1 Ma, 55.9 Ma, 33.9 Ma, 23.2 Ma, 13.8 Ma, 10.8 Ma and 7.6 Ma, the latter mainly from the $\delta^{13}C$ record. Four of them are indeed identical to those determined in the present study: 62.1 Ma, 55.9 Ma, 33.9 Ma and 13.8 Ma, the first two being preceded by a significant early warning signal (*50*) which does not appear to be the case for the EOT key transition..

2 The Past 3.2 Myr history of the Earth climate, mainly from Northern Hemisphere

As indicated previously, the last 3.3 Myr have been defined as an Icehouse climate state, with the appearance of NHIS, their development and variations through time (*26*) while Antarctic ice sheets already reached mostly their maximal expansion. This Icehouse state is characterized by a change of the interplay between benthic $\delta^{13}C$ and $\delta^{18}O$, which corresponds to a new relationship between the carbon cycle and climate (*51*).

The RQA of U1308 benthic foram $\delta^{18}O$, we have identified six steps in the $\delta^{18}O$ variability (Fig. 2, Suppl. Tab. 1). They correspond to abrupt transitions dated at 2.95 Ma, at 2.55 Ma, at 1.5 Ma, at 1.25 Ma, at 0.65 Ma and at 0.35 Ma, which characterize the dynamics of North Hemisphere ice sheets (elevation and spatial expansion). Interestingly, the interval 1.25 Ma to 0.65 Ma corresponds roughly to the previously mentioned MPT, during which a shift occurred from climate cycles dominated by a 40-Kyr periodicity to 100-Kyr dominated ones (*52–56*). The 1.25 Ma date is particularly significant, since it is followed by an increase in the amplitude of glacial–interglacial fluctuations. The $\delta^{18}O$ bulk carbonate record in the U1308 core, in turn, is interpreted as characterizing IRD released into the North Atlantic Ocean (*27*). The RQA of this record also displays a drifting regime, and it yields abrupt transitions at 2.75 Ma, at 1.5 Ma, at 1.25 Ma, at 0.9 Ma and 0.65 Ma which characterize the dynamics of NHIS through episodic to more regular and of larger magnitude iceberg calving (Supp. Fig. 2)

These abrupt transitions identified during the past 3.2 Myr occur in the Earth context where the Antarctic ice sheets are built and had already a major impact on the course of the Earth climate. Although significant, they relate to the evolution of NHIS history and therefore could be rather labeled Critical Thresholds (CT) (see Fig. 2).

3 A hierarchy of abrupt transitions

Traditionally, tipping points are schematically represented as being associated with the bifurcation occurring for a system described by a one-dimensional effective potential when a change in the value of a certain parameter leads to a change in the number of stable equilibriums. Hence, conditions describing the nearing of a tipping point can be related to the presence of slower decay of correlations (critical slowing down). This viewpoint, while attractive, suffers from many mathematical issues due to the fact that the true dynamics of the system occurs in a possibly very high dimensional space. (*57*, *58*) have introduced a mathematically rigorous framework for the occurrence of tipping points that clarifies the link between rate of decay of correlations, sensitivity of the system to perturbations, and robustness of the unperturbed dynamics.

This suggests the possibility at identifying a potential hierarchy of past critical events, which would give a more complex perspective on the history of the climate than the classical saddle-node two-dimension representation of tipping points described above. Indeed, (*59*, *60*) proposed to describe the global properties of the climate system using the formalism of (*61*) quasi-potential. The minima of such quasi-potential, which has strong similarities with the epigenetic landscape (*62–66*), correspond to local maxima of the probability distribution of the system associated with the competing climatic states, and the saddles correspond to the Melancholia states (*67*) of the system, gateways for the noise-induced transitions between such states. (*68*) suggested that the presence of decorations of the quasi-potential at different scales would lead exactly to a hierarchy of tipping points. Figure 4 illustrates such hierarchy of abrupt transitions from the $\delta^{18}O$ benthic time series. It shows that about 70-80% of the observed TPs are located in saddles of the probability density and that the same saddle is sometime crossed more than once.

Added to the Chicxulub meteor impact previously mentioned, which injected a considerable amount of CO_2 into the atmosphere (*69*, *70*), Deccan traps were already spreading at the beginning of the Cenozoic, contributing to the release of massive amount of CO_2 (*15*). CO_2 concentration continued raising until about 500 ppmv with the North Atlantic Igneous province very active at about 58 Ma - 56Ma (TP2 and TP3) in relation with the opening of the North Atlantic Ocean (*71*). The Northern Hemisphere plates were connected and not facing the present Arctic conditions allowing faunal and vegetal dispersion. Other plates were on the contrary reorganizing like India moving northeastward toward the Asian continent. Equatorial Pacific carbonate compensation depth (CCD) reached a minimum value a bit later at about 54 Ma when CO_2 concentration reached its maximum of the whole Cenozoic above 1,100 ppmv (*48*). The lowering of the GMSL and of the CCD at TP4 (about 40 Myr) has been interpreted as the start of the icing of Antarctica through mountain glaciers deposits dates by K-Ar dating of lava flows (*72*), supported by other glacial evidences i.e., from the Gamburtsev subglacial mountains (*73*), while Northern Hemisphere plates remained connected. By TP4 India is approaching the Asian plate while Northern Hemisphere ones were still connected, allowing northern continental migrations of mammals at high latitudes (*74*, *75*). At TP6, about 34 Myr, the Drake and Tasmanian passages are opening (*76*), even if several steps, inducing a drastic change in the whole deep and surficial oceanic circulation, characterized by a decrease in the South Hemisphere water

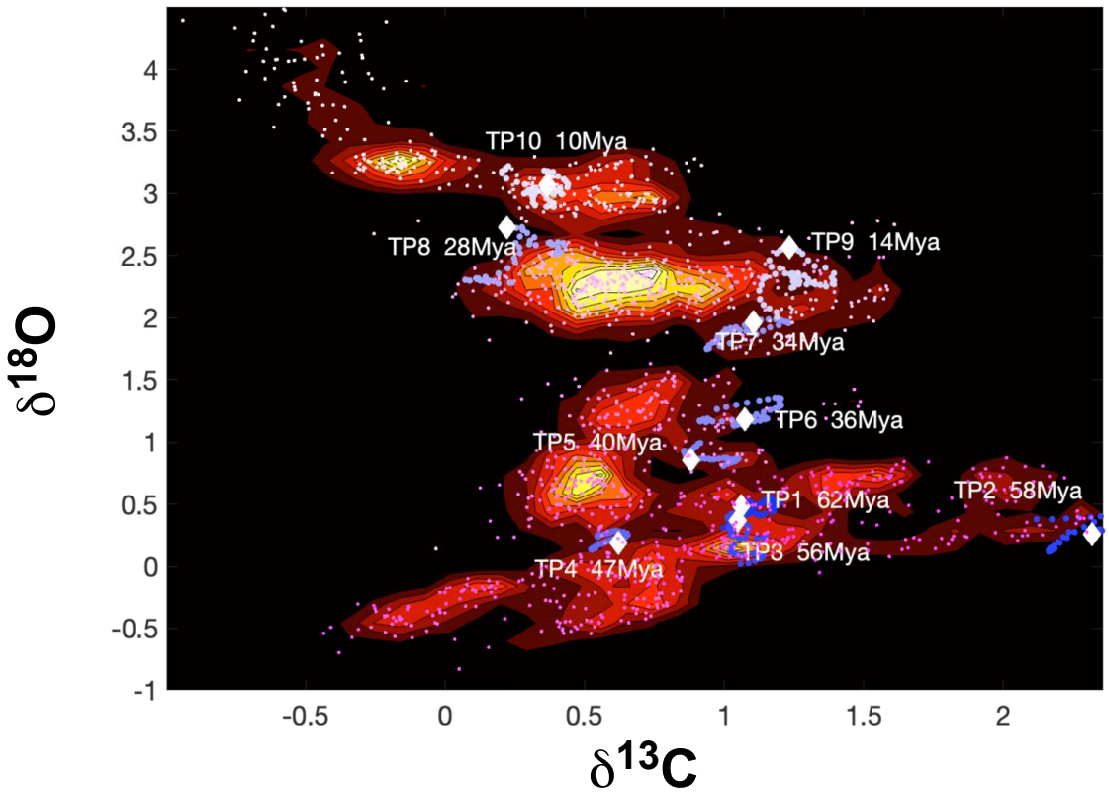

Fig. 4. **Quasi-Potential topography of the climate system in the CENOGRID benthic $\delta^{18}O$ and $\delta^{13}C$. space.** Probability Density plot with the Tipping points ordered by priority according to the recurrence analysis for $\delta^{18}O$; the approximate timing is also indicated (rounded to 1 My). 50 Kyr before and after each TP (indicated by the white diamond) is also plotted. Darker blue hues indicate that we are going to the more distant past. Each dot corresponds to 2 Kyr. One point every 50 Ky from the time series is also added; darker magenta indicate more distant past, showing the direction of evolution of the climate.

formation strength, a deep sea temperature drop associated with the deep fall in relative sea level and CCD (see Fig. 3). According to paleoaltimetry estimates based on oxygen isotopes, (*77*) indicate that the Tibetan Plateau had an elevation of about 4000m, favoring therefore the physical weathering of rocks, consuming CO_2, and the burial of carbon through high sedimentation rates in the adjacent seas. This may have contributed to the major threshold in the variation of the CO_2 concentration, which also drops very strongly ((*48*); Fig. 3).

This key transition is the major boundary between two different climate landscapes dominated by intensive plate tectonic and major volcanism for the older one, and by major ice sheets in both Southern and Northern Hemispheres, with plate tectonic (closure of seaways, orogenies) still very active, for the younger one (*75*). Immediately after the EOT, the climate witnessed the build up of the East Antarctic ice sheet (Oi-1 glaciation), which can be considered as the onset of the cold world in which we are still living. India has almost ended its transfer to the Asian plate. Between TP6 and TP 7, i.e., 34 and 14 Myr respectively, the East Antarctic ice sheet is waxing and vanning with several major glaciations occurring before the 17 Myr to 14.5 Myr interval during which sea level increases in association with a severe shoaling episode of CCD and higher

values of the CO_2 concentration (Fig. 3). Such high CO_2 concentrations may have been fueled by the Columbia River major volcanism, which ended by TP 7 at about 14 Ma (*15*). Plate tectonics is still very active with the closure of both the Indonesian gateway and the Tethyan seaway, contributing to the start of the development of the Mediterranean (*78*), and. Eurasia is now separated from Northern America and Greenland, India colliding the Asian continent, and the Andes are uplifting modifying the geometry of the marine basins and the global oceanic circulation. West Antarctica is starting building up while East Antarctic ice sheet is reinforcing and expanding. TP8 at about 9 Ma sees a strong lowering of the GMSL and of the CO_2 concentrations (Fig. 3). The final major tectonic event corresponds to the closure of the Panama Isthmus at TP9, which definitively configure the oceanic circulation close to the current one (*79*). This is associated to a strong lowering of the global sea level, a deepening of the CCD and the CO_2 concentration (Fig. 3) that will preside the Earth climate history during the Quaternary, associated to the build up of the Northern Hemisphere glaciers and ice sheets. It is interesting to notice that all the major transitions that have been identified during the interval between 66 Ma and 2.9-2.5 Ma, are linked to the build up, waxing and vanning of the Northern and Southern Hemisphere ice sheets.

Considering the results of both RQA, KS test and quasi-potential view point, a concept of a hierarchy of abrupt transitions can therefore be proposed as described in figure 5, showing the major climate transitions, TP1 to TP10, which shaped the Earth climate towards the onset and development of the Southern ice sheets and the later build up of the NHIS, impacted by critical thresholds (CT1 to CT4) which steered their development and evolution. Such evolution occurred within two different climate landscapes bounded by the 34 Ma major transition. Without the major drop in GMSL, in CO2 concentration and in CCD, the Earth climate could have been different. However passing this major threshold, the Earth climate entered a new landscape marked by much lower CO2 concentration, lower GMSL and CCD. The oceanic basin redesign and the mountain uplifts changed the marine and atmospheric circulations patterns, leading to the onset and development of the NHIS. Variations in these NHIS extent and volume have contributed to the occurrence of the millennial variability marked by the Bond cycles as better described during the last climate cycle but, which onset has been proposed to be dated of 0.9 Ma (*12*).

This succession of abrupt transitions characterizes a domino-like effect leading the Earth System to pass from one climate landscape to another under the natural regulation of the

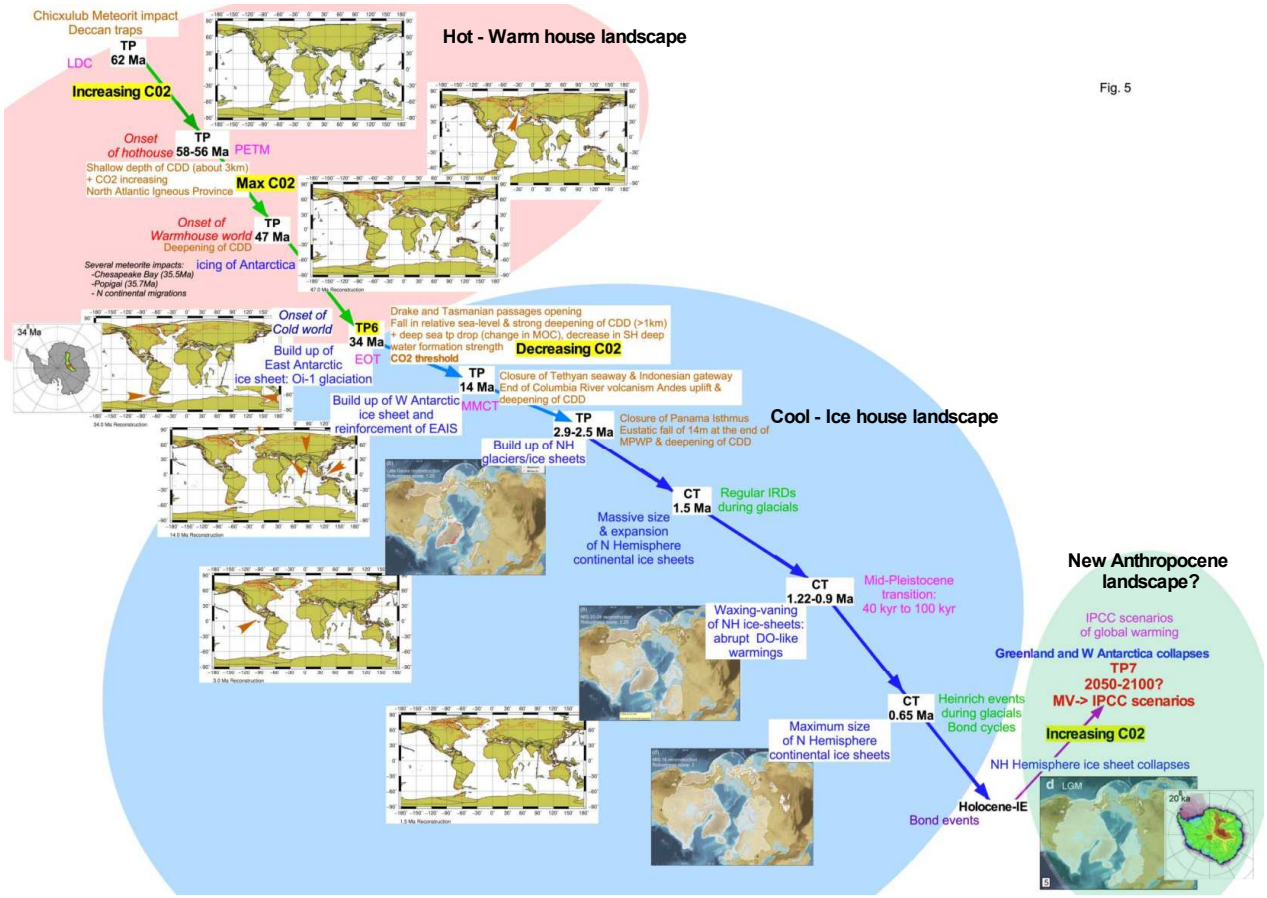

Fig. 5

Fig. 5. **Evolution of the Earth Climate history among 2 different tipping landscapes and proposal for a potential third one.** The first landscape in light red, corresponds to the Hot-Warm House time interval. The second landscape in light blue corresponds to the Cold-Ice house time interval. The third landscape, in light green, corresponds to the potential new one represented by the Anthropocene time interval. The different abrupt transitions identified in the present study are reported as TP or CT to differentiate the major tipping points from the critical transitions characterizing transitions of lighter significance in the climate history. Various plate tectonic and ice sheet events are indicated and supported by maps of plate movements and North and South Hemisphere ice sheets. The Antarctica maps are from (*86*), Northern Hemisphere ice sheet maps are from (*87*). The paleogeographic maps have been generated using the Ocean Drilling Stratigraphic Network (ODSN) plate tectonic reconstruction service: < https://www.odsn.de/odsn/services/paleomap/paleomap.html>. The red arrows on the tectonic maps indicate the key events at the identified abrupt transition.

astronomical parameters (Fig. 5, see Supplementary material). However, a new and unexpected future abrupt transition has to be considered with high confidence as noticed by instrumental observations impacting numerous tipping elements (see (*17*) through very drastic tipping cascades (*19*). This potential upcoming major transition does not seem to follow the previous succession of CT observed during the past 2.9 Myr and maintaining the climate variability within the same climate landscape. This potential major transition rather could be the boundary between the Cenozoic icehouse tipping landscape and another new one corresponding to the strong variations in key climate factors induced by the human activity. Indeed, IPCC reports and other published evidences are demonstrating that both climate and biodiversity seem evolving towards possible irreversible changes, making this upcoming abrupt transition a major tipping

point in the Earth System, similar to TP6 at 34 Ma, involving perhaps new parameters to be considered, but also leading to a new and unknown climate landscape (Fig. 5).

Methods

The augmented Kolmogorov-Smirnov test is a robust method for finding local maxima and minima in a particular time series and is therefore a very precise way for timing the onset of abrupt transitions successfully applied to various geological time series. The method compares two samples taken before and after the potential transition point to test whether they come from the same continuous distribution. If they do not, the transition point is identified as a significant abrupt change indicative of a true climatic shift. (see for more details (*12*, *28*))

To gain further insight like recurring patterns into the climate story the records tell us, we performed a quantitative, objective analysis of these time series of proxy variables, based on the recurrence plots (RPs) introduced by (*80*) into the study of dynamical systems and popularized in the climate sciences by (*31*, *81*). The RP for a time series $\{x_i: i = 1, \ldots, N\}$ is constructed as a square matrix in a cartesian plane with the abscissa and ordinate both corresponding to a time-like axis, with one copy $\{x_i\}$ of the series on the abscissa and another copy $\{x_j\}$ on the ordinate. A dot is entered into a position (i, j) of the matrix when x_j is sufficiently close to x_i. For the details — such as how "sufficiently close" is determined — we refer to (*80*) and (*81*). All the points on the diagonal $i = j$ have dots and, in general, the matrix is rather symmetric, although one does not always define closeness symmetrically; to wit, x_j may be "closer to" x_i than x_i is to x_j (*80*). An important advantage of the RP method is that it does apply to dynamical systems that are not autonomous, i.e., that may be subject to time-dependent forcing. The latter is certainly the case for the climate system on time scales of 10–100 Kyr and longer, which is affected strongly by orbital forcing.

(*80*) distinguished between large-scale *typology* and small-scale *texture* in the interpretation of square matrix of dots that is the visual result of RP. Thus, if all the characteristic times of an autonomous dynamical system are short compared to the length of the time series, the RP's typology will be homogeneous and, thus, not very interesting. In the presence of an imposed drift, a more interesting typology will appear. The most interesting typology in RP applications so far is associated with recurrent patterns that are not exactly periodic but only nearly so. Hence, such patterns are not that easily detectable by purely spectral approaches to time series analysis. (*81*) discussed how to render the purely visual RP typologies studied up to that point more objectively quantifiable by recurrence quantification analysis and bootstrapping (*82*, *83*). The RP

exhibits, moreover, a characteristic texture — given by the pattern of vertical and horizontal lines that mark recurrences. These lines sometimes form recurrence clusters that correspond to specific periodic patterns.

The quasi-potential landscape analysis has been developed to visualize the state space of a time series through troughs, characterizing stable climate states, and ridges characterizing unstable climate conditions with local maxima corresponding to saddles, which are potential transitions from one basin to another. (*84*) give a complete overview of different methods applied to perform such analysis. Moreover (*68*) described elegantly the potential of such analysis by applying it to the computations performed with the PLASIM intermediate complexity climate model.

References

1. W. Dansgaard, S. J. Johnsen, J. Moller, C. C. Langway, One thousand centuries of climatic record from Camp Century on the Greenland ice sheet. *Science*. **166**, 377–381 (1969).
2. W. Dansgaard, H. B. Clausen, N. Gundestrup, C. U. J. Hammer, S. F. ohnsen, P. M. Kristinsdottir, N. Reeh, A new Greenland deep ice core. *Science*. **218**, 1273–1277 (1982).
3. W. Broecker, Climatic Change - Are we on the brink of a pronounced global warming. *Science*. **189**, 460–463 (1975).
4. W. S. Broecker, M. Andree, G. Bonani, W. Wolfi, H. Oeschger, M. Klas, Can the Greenland climatic jumps be identified in records from ocean and land? *Quat. Res.* **30**, 1–6 (1988).
5. W. S. Broecker, G. Denton, The role of ocean-atmosphere reorganizations in glacial cycles. *Geochim Cosmochim Acta*. **53**, 2465–2501 (1989).
6. S. O. Rasmussen, M. Bigler, S. P. Blockley, T. Blunier, S. L. Buchardt, H. B. Clausen, I. Cvijanovic, D. Dahl-Jensen, S. J. Johnsen, H. Fischer, V. Gkinis, M. Guillevic, W. Z. Hoek, J. J. Lowe, J. B. Pedro, T. Popp, I. K. Seierstad, J. P. Steffensen, A. M. Svensson, P. Vallelonga, B. M. Vinther, M. J. C. Walker, J. J. Wheatley, M. Winstrup, A stratigraphic framework for abrupt climatic changes during the Last Glacial period based on three synchronized Greenland ice-core records: refining and extending the INTIMATE event stratigraphy. *Quat. Sci. Rev.* **106**, 14–28 (2014).
7. G. Bond, H. Heinrich, W. Broecker, L. Labeyrie, J. McManus, J. Andrews, S. Huon, R. Jantschik, S. Clasen, C. Simet, K. Tedesco, M. Klas, G. Bonani, S. Ivy, Evidence for massive discharges of icebergs into the North Atlantic Ocean during the

last glacial period. *Nature*. **360**, 245–249 (1992).

8. Y. J. Wang, H. Cheng, R. L. Edwards, Z. S. An, J. Y. Wu, C. C. Shen, J. A. Dorale, A high-resolution absolute-dated Late Pleistocene monsoon record from Hulu Cave, China. *Science*. **294**, 2345–2348 (2001).
9. S. Barker, G. Knorr, R. L. Edwards, F. Parrenin, A. E. Putnam, L. C. Skinner, E. Wolff, M. Ziegler, 800,000 Years of Abrupt Climate Variability. *Science*. **334**, 347–351 (2011).
10. H. Cheng, R. L. Edwards, A. Sinha, C. Spotl, L. Yi, S. T. Chen, M. Kelly, G. Kathayat, X. F. Wang, X. L. Li, X. G. Kong, Y. J. Wang, Y. F. Ning, H. W. Zhang, The Asian monsoon over the past 640,000 years and ice age terminations. *Nature*. **534**, 640–646 (2016).
11. D.-D. Rousseau, P. Antoine, N. Boers, F. Lagroix, M. Ghil, J. Lomax, M. Fuchs, M. Debret, C. Hatté, O. Moine, C. Gauthier, D. Jordanova, N. Jordanova, Dansgaard-Oeschger-like events of the penultimate climate cycle: The loess point of view. *Clim. Past*. **16**, 713–727 (2020).
12. D. Rousseau, W. Bagniewski, M. Ghil, Abrupt climate changes and the astronomical theory: are they related? *Clim. Past*. **18**, 249–271 (2022).
13. B. Birner, D. A. Hodell, P. C. Tzedakis, L. C. Skinner, Similar millennial climate variability on the Iberian margin during two early Pleistocene glacials and MIS 3. *Paleoceanography*. **31**, 203–217 (2016).
14. P. F. Hoffman, D. S. Abbot, Y. Ashkenazy, D. I. Benn, J. J. Brocks, P. A. Cohen, G. M. Cox, J. R. Creveling, Y. Donnadieu, D. H. Erwin, I. J. Fairchild, D. Ferreira, J. C. Goodman, G. P. Halverson, M. F. Jansen, G. Le Hir, G. D. Love, F. A. Macdonald, A. C. Maloof, C. A. Partin, G. Ramstein, B. E. J. Rose, C. V. Rose, P. M. Sadler, E. Tziperman, A. Voigt, S. G. Warren, Snowball Earth climate dynamics and Cryogenian geology-geobiology. *Sci. Adv.* **3** (2017), doi:10.1126/sciadv.1600983.
15. C. R. Scotese, H. Song, B. J. W. Mills, D. G. van der Meer, Phanerozoic paleotemperatures: The earth's changing climate during the last 540 million years. *Earth-Sci. Rev.* **215** (2021), doi:10.1016/j.earscirev.2021.103503.
16. T. Lenton, H. Held, E. Kriegler, J. Hall, W. Lucht, S. Rahmstorf, H. Schellnhuber, Tipping elements in the Earth's climate system. *Proc. Natl. Acad. Sci. U. S. A.* **105**, 1786–1793 (2008).
17. T. Lenton, "Environmental Tipping Points" in *Annual review of Environment and Resources*, A. Gadgil, D. Liverman, Eds. (2013), vol. 38, pp. 1–29.
18. T. Lenton, J. Rockstrom, O. Gaffney, S. Rahmstorf, K. Richardson, W. Steffen, H. Schellnhuber, Climate tipping points - too risky to bet against. *Nature*. **575**, 592–595

(2019).

19. V. Brovkin, E. Brook, J. Williams, S. Bathiany, T. Lenton, M. Barton, R. DeConto, J. Donges, A. Ganopolski, J. McManus, S. Praetorius, A. de Vernal, A. Abe-Ouchi, H. Cheng, M. Claussen, M. Crucifix, G. Gallopin, V. Iglesias, D. Kaufman, T. Kleinen, F. Lambert, S. van der Leeuw, H. Liddy, M. Loutre, D. McGee, K. Rehfeld, R. Rhodes, A. Seddon, M. Trauth, L. Vanderveken, Z. Yu, Past abrupt changes, tipping points and cascading impacts in the Earth system. *Nat. Geosci.* **14**, 550–558 (2021).
20. T. Lenton, H. Williams, On the origin of planetary-scale tipping points. *Trends Ecol. Evol.* **28**, 380–382 (2013).
21. W. Steffen, J. Rockstrom, K. Richardson, T. Lenton, C. Folke, D. Liverman, C. Summerhayes, A. Barnosky, S. Cornell, M. Crucifix, J. Donges, I. Fetzer, S. Lade, M. Scheffer, R. Winkelmann, H. Schellnhuber, Trajectories of the Earth System in the Anthropocene. *Proc. Natl. Acad. Sci. U. S. A.* **115**, 8252–8259 (2018).
22. E. Kriegler, J. Hall, H. Held, R. Dawson, H. Schellnhuber, Imprecise probability assessment of tipping points in the climate system. *Proc. Natl. Acad. Sci. U. S. A.* **106**, 5041–5046 (2009).
23. N. Wunderling, J. Donges, J. Kurths, R. Winkelmann, Interacting tipping elements increase risk of climate domino effects under global warming. *Earth Syst. Dyn.* **12**, 601–619 (2021).
24. I. Otto, J. Donges, R. Cremades, A. Bhowmik, R. Hewitte, W. Lucht, J. Rockstrom, F. Allerberger, M. McCaffrey, S. Doe, A. Lenferna, N. Moran, D. van Vuuren, H. Schellnhuber, Social tipping dynamics for stabilizing Earth's climate by 2050. *Proc. Natl. Acad. Sci. U. S. A.* **117**, 2354–2365 (2020).
25. T. Lenton, S. Benson, T. Smith, T. Ewer, V. Lanel, E. Petykowski, T. Powell, J. Abrams, F. Blomsma, S. Sharpe, Operationalising positive tipping points towards global sustainability. *Glob. Sustain.* **5** (2022), doi:10.1017/sus.2021.30.
26. T. Westerhold, N. Marwan, A. J. Drury, D. Liebrand, C. Agnini, E. Anagnostou, J. S. K. Barnet, S. M. Bohaty, D. De Vleeschouwer, F. Florindo, T. Frederichs, D. A. Hodell, A. E. Holbourn, D. Kroon, V. Lauretano, K. Littler, L. J. Lourens, M. Lyle, H. Palike, U. Rohl, J. Tian, R. H. Wilkens, P. A. Wilson, J. C. Zachos, An astronomically dated record of Earth's climate and its predictability over the last 66 million years. *Science*. **369**, 1383-+ (2020).
27. D. A. Hodell, J. E. T. Channell, Mode transitions in Northern Hemisphere glaciation: co-evolution of millennial and orbital variability in Quaternary climate. *Clim. Past*. **12**, 1805–1828 (2016).
28. W. Bagniewski, M. Ghil, D. D. Rousseau, Automatic detection of abrupt transitions

in paleoclimate records. *Chaos*. **31** (2021), doi:10.1063/5.0062543.

29. J. Zachos, M. Pagani, L. Sloan, E. Thomas, K. Billups, Trends, rhythms, and aberrations in global climate 65 Ma to present. *Science*. **292**, 686–693 (2001).

30. J. Zachos, J. Breza, S. Wise, Early Oligocene ice-sheet expansion on Antractica - stable isotope and sedimentological evidence from Kerguelen Plateau, Southern Indian-Ocean. *Geology*. **20**, 569–573 (1992).

31. N. Marwan, M. Carmen Romano, M. Thiel, J. Kurths, Recurrence plots for the analysis of complex systems. *Phys. Rep.* **438**, 237–329 (2007).

32. E. Thomas, J. C. Zachos, T. J. Bralower, "Deep-sea environments on a warm earth: latest Paleocene-early Eocene" in *Warm Climates in Earth History*, B. T. Huber, K. G. Macleod, S. L. Wing, Eds. (Cambridge University Press, Cambridge, 1999; https://www.cambridge.org/core/books/warm-climates-in-earth-history/deepsea-environments-on-a-warm-earth-latest-paleoceneearly-eocene/5812213E2DDEB85D28B654244C4ECE86), pp. 132–160.

33. K. Miller, J. Browning, W. Schmelz, R. Kopp, G. Mountain, J. Wright, Cenozoic sea-level and cryospheric evolution from deep-sea geochemical and continental margin records. *Sci. Adv.* **6** (2020), doi:10.1126/sciadv.aaz1346.

34. J. Kennett, L. Stott, Abrupt deep-sea warming, palaeoceanographic changes and benthic extinctions at the end of the Paleocene. *Nature*. **353**, 225–229 (1991).

35. G. R. Dickens, M. M. Castillo, J. C. Walker, A blast of gas in the latest Paleocene: simulating first-order effects of massive dissociation of oceanic methane hydrate. *Geology*. **25 3**, 259–62 (1997).

36. J. Kennett, N. Shackleton, Oxugen isotopic evidence for development of psychrosphere 38 Myr ago. *Nature*. **260**, 513–515 (1976).

37. N. J. Shackleton, "Oceanic Carbon Isotope Constraints on Oxygen and Carbon Dioxide in the Cenozoic Atmosphere" in *The Carbon Cycle and Atmospheric CO2: Natural Variations Archean to Present* (American Geophysical Union (AGU), 1985; https://agupubs.onlinelibrary.wiley.com/doi/abs/10.1029/GM032p0412), pp. 412–417.

38. J. Chappell, N. J. Shackleton, Oxygen isotopes and sea-level. *Nature*. **324**, 137–140 (1986).

39. N. J. Shackleton, The 100,000-year ice-age cycle identified and found to lag temperature, carbon dioxide, and orbital eccentricity. *Science*. **289**, 1897–1902 (2000).

40. H. Elderfield, P. Ferretti, M. Greaves, S. Crowhurst, I. N. McCave, D. Hodell, A. M. Piotrowski, Evolution of Ocean Temperature and Ice Volume Through the Mid-Pleistocene Climate Transition. *Science*. **337**, 704–709 (2012).

41. M. Milankovic, *Théorie mathématique des Phénomènes thermiques produits par la*

radiation solaire (Gauthier Villars, Paris, 1920).

42. M. Milankovic, *Kanon der Erdbestrahlung und seine Anwendung auf das Eiszeitenproblem* (Royal Serbian Sciences, Belgrade, 1941), *Special publication*.

43. S. Gulick, P. Barton, G. Christeson, J. Morgan, M. McDonald, K. Mendoza-Cervantes, Z. Pearson, A. Surendra, J. Urrutia-Fucugauchi, P. Vermeesch, M. Warner, Importance of pre-impact crustal structure for the asymmetry of the Chicxulub impact crater. *Nat. Geosci.* **1**, 131–135 (2008).

44. S. Gulick, G. Christeson, P. Barton, R. Grieve, J. Morgan, J. Urrutia-Fucugauchi, Geophysical characterization of the Chicxulub impact crater. *Rev. Geophys.* **51**, 31–52 (2013).

45. S. Gulick, A. Shevenell, A. Montelli, R. Fernandez, C. Smith, S. Warny, S. Bohaty, C. Sjunneskog, A. Leventer, B. Frederick, D. Blankenship, Initiation and long-term instability of the East Antarctic Ice Sheet. *Nature*. **552**, 225-+ (2017).

46. S. Gulick, T. Bralowe, J. Ormo, B. Hall, K. Grice, B. Schaefer, S. Lyons, K. Freeman, J. Morgan, N. Artemieva, P. Kaskes, S. de Graaff, M. Whalen, G. Collins, S. Tikoo, C. Verhagen, G. Christeson, P. Claeys, M. Coolen, S. Goderis, K. Goto, R. Grieve, N. McCall, G. Osinski, A. Rae, U. Biller, J. Smit, V. Vajda, A. Wittmann, Expedition 364 Scientists, The first day of the Cenozoic. *Proc. Natl. Acad. Sci. U. S. A.* **116**, 19342–19351 (2019).

47. H. Palike, M. Lyle, H. Nishi, I. Raffi, A. Ridgwell, K. Gamage, A. Klaus, G. Acton, L. Anderson, J. Backman, J. Baldauf, C. Beltran, S. Bohaty, P. Bown, W. Busch, J. Channell, C. Chun, M. Delaney, P. Dewangan, T. Dunkley Jones, K. Edgar, H. Evans, P. Fitch, G. Foster, N. Gussone, H. Hasegawa, E. Hathorne, H. Hayashi, J. Herrle, A. Holbourn, S. Hovan, K. Hyeong, K. Iijima, T. Ito, S. Kamikuri, K. Kimoto, J. Kuroda, L. Leon-Rodriguez, A. Malinverno, T. Moore, B. Murphy, D. Murphy, H. Nakamura, K. Ogane, C. Ohneiser, C. Richter, R. Robinson, E. Rohling, O. Romero, K. Sawada, H. Scher, L. Schneider, A. Sluijs, H. Takata, J. Tian, A. Tsujimoto, B. Wade, T. Westerhold, R. Wilkens, T. Williams, P. Wilson, Y. Yamamoto, S. Yamamoto, T. Yamazaki, R. Zeebe, A Cenozoic record of the equatorial Pacific carbonate compensation depth. *Nature*. **488**, 609-+ (2012).

48. D. Beerling, D. Royer, Convergent Cenozoic CO2 history. *Nat. Geosci.* **4**, 418–420 (2011).

49. IPCC, *Climate Change 2021: The Physical Science Basis. Contribution of Working Group I to the Sixth Assessment Report of the Intergovernmental Panel on Climate Change* (Cambridge University Press, Cambridge, United Kingdom and New York, NY, USA, 2021), vol. In Press.

50. C. Boettner, G. Klinghammer, N. Boers, T. Westerhold, N. Marwan, Early-warning signals for Cenozoic climate transitions. *Quat. Sci. Rev.* **270** (2021), doi:10.1016/j.quascirev.2021.107177.
51. S. K. Turner, Pliocene switch in orbital-scale carbon cycle/climate dynamics. *Paleoceanography*. **29**, 1256–1266 (2014).
52. N. J. Shackleton, N. D. Opdyke, Oxygen isotope and palaeomagnetic evidence for early Northern Hemisphere glaciation. *Nature*. **270**, 216–223 (1977).
53. N. G. Pisias, T. C. Moore, The evolution of Pleistocene climate: A time-series approach. *Earth Planet. Sci. Lett.* **52**, 450–458 (1981).
54. W. F. Ruddiman, M. Raymo, D. G. Martinson, B. M. Clement, J. Backman, Pleistocene evolution : Northern Hemisphere ice sheets and North Atlantic Ocean. *Paleoceanography,*. **4**, 353–412 (1989).
55. P. U. Clark, D. Pollard, Origin of the middle Pleistocene transition by ice sheet erosion of regolith. *Paleoceanography*. **13**, 1–9 (1998).
56. P. U. Clark, D. Archer, D. Pollard, J. D. Blum, J. A. Rial, V. Brovkin, A. C. Mix, N. G. Pisias, M. Roy, The middle Pleistocene transition: characteristics. mechanisms, and implications for long-term changes in atmospheric PCO2. *Quat. Sci. Rev.* **25**, 3150–3184 (2006).
57. A. Tantet, V. Lucarini, H. Dijkstra, Resonances in a Chaotic Attractor Crisis of the Lorenz Flow. *J. Stat. Phys.* **170**, 584–616 (2018).
58. A. Tantet, V. Lucarini, F. Lunkeit, H. Dijkstra, Crisis of the chaotic attractor of a climate model: a transfer operator approach. *Nonlinearity*. **31**, 2221–2251 (2018).
59. V. Lucarini, T. Bodai, Transitions across Melancholia States in a Climate Model: Reconciling the Deterministic and Stochastic Points of View. *Phys. Rev. Lett.* **122** (2019), doi:10.1103/PhysRevLett.122.158701.
60. V. Lucarini, T. Bodai, Global stability properties of the climate: Melancholia states, invariant measures, and phase transitions. *Nonlinearity*. **33**, R59–R92 (2020).
61. R. Graham, "Macroscopic potentials, bifurcations and noise in dissipative systems" in *Fluctuations and stochastic phenomena in condensed matter* (Springer, 1987), pp. 1–34.
62. C. H. Waddington, Canalization of development and the inheritance of acquired characters. *Nature*. **150**, 563–565 (1942).
63. C. H. Waddington, *The strategy of the genes.* (Allen & Unwin., London, 1957).
64. A. D. Goldberg, C. D. Allis, E. Bernstein, Epigenetics: a landscape takes shape. *Cell*. **128**, 635–638 (2007).
65. J. Baedke, The epigenetic landscape in the course of time: Conrad Hal

Waddington's methodological impact on the life sciences. *Stud. Hist. Philos. Sci. Part C Stud. Hist. Philos. Biol. Biomed. Sci.* **44**, 756–773 (2013).

66. M. Allen, Compelled by the diagram: thinking through CH Waddington's epigenetic landscape. *Contemporaneity*. **4**, 119 (2015).

67. V. Lucarini, T. Bodai, Edge states in the climate system: exploring global instabilities and critical transitions. *Nonlinearity*. **30**, R32–R66 (2017).

68. G. Margazoglou, T. Grafke, A. Laio, V. Lucarini, Dynamical landscape and multistability of a climate model. *Proc. R. Soc. -Math. Phys. Eng. Sci.* **477** (2021), doi:10.1098/rspa.2021.0019.

69. J. D. O'Keefe, T. J. Ahrens, Impact production of C02 by the Cretaceous/Tertiary extinction bolide and the resultant heating of the Earth. *Nature*. **338**, 247–249 (1989).

70. B. Lomax, D. Beerling, G. Upchurch, B. Otto-Bliesner, Rapid (10-yr) recovery of terrestrial productivity in a simulation study of the terminal Cretaceous impact event. *Earth Planet. Sci. Lett.* **192**, 137–144 (2001).

71. D. W. Jolley, B. R. Bell, "The North Atlantic Igneous Province: Stratigraphy, Tectonic, Volcanic, and Magmatic Processes" in (Geological Society of London, 2002).

72. K. Birkenmajer, A. Gaździcki, K. P. Krajewski, A. Przybycin, A. Solecki, A. Tatur, H. I. Yoon, First Cenozoic glaciers in west Antarctica. *Pol. Polar Res.*, 3-12-3–12 (2005).

73. K. Rose, F. Ferraccioli, S. Jamieson, R. Bell, H. Corr, T. Creyts, D. Braaten, T. Jordan, P. Fretwell, D. Damaske, Early East Antarctic Ice Sheet growth recorded in the landscape of the Gamburtsev Subglacial Mountains. *Earth Planet. Sci. Lett.* **375**, 1–12 (2013).

74. C. Janis, Tertiary mammal evolution in the context of changing climates, vegetation, and tectonic events. *Annu. Rev. Ecol. Syst.* **24**, 467–500 (1993).

75. T. H. Torsvik, L. R. M. Cocks, *Earth history and palaeogeography* (Cambridge University Press, 2016).

76. Y. Lagabrielle, Y. Godderis, Y. Donnadieu, J. Malavieille, M. Suarez, The tectonic history of Drake Passage and its possible impacts on global climate. *Earth Planet. Sci. Lett.* **279**, 197–211 (2009).

77. D. Rowley, B. Currie, Palaeo-altimetry of the late Eocene to Miocene Lunpola basin, central Tibet. *Nature*. **439**, 677–681 (2006).

78. O. Bialik, M. Frank, C. Betzler, R. Zammit, N. Waldmann, Two-step closure of the Miocene Indian Ocean Gateway to the Mediterranean. *Sci. Rep.* **9** (2019), doi:10.1038/s41598-019-45308-7.

79. D. Lunt, P. Valdes, A. Haywood, I. Rutt, Closure of the Panama Seaway during the Pliocene: implications for climate and Northern Hemisphere glaciation. *Clim. Dyn.* **30**, 1–18 (2008).

80. J. P. Eckmann, S. O. Kamphorst, D. Ruelle, Recurrence plots of dynamical systems. *Europhys. Lett.* **4**, 973–977 (1987).

81. N. Marwan, S. Schinkel, J. Kurths, Recurrence plots 25 years later - Gaining confidence in dynamical transitions. *EPL*. **101** (2013), doi:10.1209/0295-5075/101/20007.

82. B. Efron, nonparametric estimates of standard error - The Jackknife, the bootstrap and other methods. *Biometrika*. **68**, 589–599 (1981).

83. B. Efron, R. Tibshirani, Bootstrap methods for standard errors, confidence intervals, and other measures of statistical accuracy. *Stat. Sci.* **1**, 54–75 (1986).

84. J. X. Zhou, M. D. S. Aliyu, E. Aurell, S. Huang, Quasi-potential landscape in complex multi-stable systems. *J. R. Soc. Interface*. **9**, 3539–3553 (2012).

85. R. DeConto, D. Pollard, P. Wilson, H. Palike, C. Lear, M. Pagani, Thresholds for Cenozoic bipolar glaciation. *Nature*. **455**, 652-U52 (2008).

86. D. Pollard, R. DeConto, Continuous simulations over the last 40 million years with a coupled Antarctic ice sheet-sediment model. *Palaeoclimatol. Palaeoecol. Palaeogeogr.* **537** (2020), doi:10.1016/j.palaeo.2019.109374.

87. C. L. Batchelor, M. Margold, M. Krapp, D. Murton, A. S. Dalton, P. L. Gibbard, C. R. Stokes, J. B. Murton, A. Manica, The configuration of Northern Hemisphere ice sheets through the Quaternary. *Nat. Commun.* **10** (2019), doi:10.1038/s41467-019-11601-2.

88. K. Miller, J. Wright, R. Fairbanks, Unlocking the ice-house Oligocene-Miocene oxygen isotopes, eustasy, and margin erosion. *J. Geophys. Res.-Solid Earth Planets*. **96**, 6829–6848 (1991).

89. S. Boulila, B. Galbrun, K. Miller, S. Pekar, J. Browning, J. Laskar, J. Wright, On the origin of Cenozoic and Mesozoic “third-order” eustatic sequences. *Earth-Sci. Rev.* **109**, 94–112 (2011).

90. G. Paxman, S. Jamieson, K. Hochmuth, K. Gohl, M. Bentley, G. Leitchenkov, F. Ferraccioli, Reconstructions of Antarctic topography since the Eocene-Oligocene boundary. *Palaeoclimatol. Palaeoecol. Palaeogeogr.* **535** (2019), doi:10.1016/j.palaeo.2019.109346.

91. E. Rohling, J. Yu, D. Heslop, G. Foster, B. Opdyke, A. Roberts, Sea level and deep-sea temperature reconstructions suggest quasi-stable states and critical transitions over the past 40 million years. *Sci. Adv.* **7** (2021), doi:10.1126/sciadv.abf5326.

92. A. Houben, C. van Mourik, A. Montanari, R. Coccioni, H. Brinkhuis, The Eocene-Oligocene transition: Changes in sea level, temperature or both? *Palaeoclimatol. Palaeoecol. Palaeogeogr.* **335**, 75–83 (2012).

93. Y. Smith, D. Hill, A. Dolan, A. Haywood, H. Dowsett, B. Risebrobakken, Icebergs in the Nordic Seas Throughout the Late Pliocene. *Paleoceanogr. Paleoclimatology*. **33**, 318–335 (2018).

94. I. Bailey, G. Hole, G. Foster, P. Wilson, C. Storey, C. Trueman, M. Raymo, An alternative suggestion for the Pliocene onset of major northern hemisphere glaciation based on the geochemical provenance of North Atlantic Ocean ice-rafted debris. *Quat. Sci. Rev.* **75**, 181–194 (2013).

95. B. D. A. Naafs, J. Hefter, R. Stein, Millennial-scale ice rafting events and Hudson Strait Heinrich(-like) Events during the late Pliocene and Pleistocene: a review. *Quat. Sci. Rev.* **80**, 1–28 (2013).

96. R. S. W. van de Wal, B. de Boer, L. J. Lourens, P. Koehler, R. Bintanja, Reconstruction of a continuous high-resolution CO2 record over the past 20 million years. *Clim. Past*. **7**, 1459–1469 (2011).

97. K. A. Jakob, P. A. Wilson, J. Pross, T. H. G. Ezard, J. Fiebig, J. Repschlager, O. Friedrich, A new sea-level record for the Neogene/Quaternary boundary reveals transition to a more stable East Antarctic Ice Sheet. *Proc. Natl. Acad. Sci. U. S. A.* **117**, 30980–30987 (2020).

98. G. Muttoni, C. Carcano, E. Garzanti, M. Ghielmi, A. Piccin, R. Pini, S. Rogledi, D. Sciunnach, Onset of major Pleistocene glaciations in the Alps. *Geology*. **31**, 989–992 (2003).

99. M. F. Knudsen, J. Norgaard, R. Grischott, F. Kober, D. L. Egholm, T. M. Hansen, J. D. Jansen, New cosmogenic nuclide burial-dating model indicates onset of major glaciations in the Alps during Middle Pleistocene Transition. *Earth Planet. Sci. Lett.* **549** (2020), doi:10.1016/j.epsl.2020.116491.

100. C. J. Berends, B. de Boer, R. S. W. van de Wal, Reconstructing the evolution of ice sheets, sea level, and atmospheric CO2 during the past 3.6 million years. *Clim. Past*. **17**, 361–377 (2021).

101. O. Seki, G. L. Foster, D. N. Schmidt, A. Mackensen, K. Kawamura, R. D. Pancost, Alkenone and boron-based Pliocene pCO(2) records. *Earth Planet. Sci. Lett.* **292**, 201–211 (2010).

102. W. S. Broecker, J. van Donk, Insolation changes, ice volumes, and 0-18 record in deep-sea cores. *Rev. Geophys. Space Phys.* **8**, 169–198 (1970).

103. J. F. McManus, D. W. Oppo, J. L. Cullen, A 0,5-million-year record of

millennial-scale climate variability in the North Atlantic. *Science*. **283**, 971–975 (1999).

104. H. Heinrich, Origin and Consequences of Cyclic Ice Rafting in the Northeast Atlantic Ocean during the Past 130,000 years. *Quat. Res.* **29**, 142–152 (1988).

105. G. Bond, W. Broecker, S. Johnsen, J. McManus, L. Labeyrie, J. Jouzel, G. Bonani, Correlations between climate records from North Atlantic sediments and Greenland ice. *Nature*. **365**, 143–147 (1993).

106. S. P. Obrochta, T. J. Crowley, J. E. T. Channell, D. A. Hodell, P. A. Baker, A. Seki, Y. Yokoyama, Climate variability and ice-sheet dynamics during the last three glaciations. *Earth Planet. Sci. Lett.* **406**, 198–212 (2014).

107. J. Jouzel, V. Masson-Delmotte, O. Cattani, G. Dreyfus, S. Falourd, G. Hoffmann, B. Minster, J. Nouet, J. Barnola, J. Chappellaz, H. Fischer, J. Gallet, S. Johnsen, M. Leuenberger, L. Loulergue, D. Luethi, H. Oerter, F. Parrenin, G. Raisbeck, D. Raynaud, A. Schilt, J. Schwander, E. Selmo, R. Souchez, R. Spahni, B. Stauffer, J. Steffensen, B. Stenni, T. Stocker, J. Tison, M. Werner, E. Wolff, Orbital and millennial Antarctic climate variability over the past 800,000 years. *Science*. **317**, 793–796 (2007).

Acknowledgments

We would like to thank our colleagues from TiPES project for fruitful discussions about this study. This is LDEO contribution and TiPES contribution XXX.

Funding:

This research has been supported by the European Commission, Horizon 2020 Framework Programme (TiPES, grant no. 820970).

Author contributions:

Conceptualization: DDR
Methodology: DDR, VL, WB
Investigation: DDR, VL, WB
Visualization: DDR, VL, WB
Writing—original draft: DDR
Writing—review & editing: DDR, VL, WB

Competing interests: All authors declare they have no competing interests.

Data and materials availability: All data generated by the present study from the main text or the supplementary materials will be submitted to PANGAEA data repository. U1308 marine data are available at https://doi.org/10.1594/PANGAEA.871937 (Hodell and Channell, 2016b). CENOGRID data are available at https://doi.org/10.1594/PANGAEA.917503 (Westerhold, 2020).

Figures and Tables

Fig. 1. **KS test and Recurrence Quantitative Analysis (RQA) of CENOGRID benthic $\delta^{18}O$.** A) Time series in Ma BP with difference of the reconstructed and present Mean Global Temperature in pink). KS test identifying abrupt transitions towards warmer conditions in red and cooler or colder conditions in blue; B) Recurrence plot (RP) with identification of the main two clusters prior and after 34 Ma. The main abrupt transitions identified are highlighted by red circles, and C) Recurrence rate (RR). The pink crosses and vertical green lines indicate the abrupt transitions (TP) detected by the RQA. CENOGRID benthic $\delta^{18}O$ data are from (*26*)

Fig. 2. **RQA of U1308 benthic $\delta^{18}O$.** A) Time series in Ma; B) RP; and C) RR. Crosses similar than Fig. S1. TP9-10 and CT1-4 abrupt transitions identified in the RR. U1308 benthic $\delta^{18}O$ data are from (*27*)

Fig. 3; **Variation through time of three main climate factors and comparison with the identified abrupt transitions (TP) in the CENOGRID benthic $\delta^{18}O$.** A) Global Mean Sea Level in meters from (*33*). Identification of particular warm and of glaciation events. The Laurentide, GIW-WAIS and Ice free lines are from (*33*); B) Carbonate Compensation Depth (CCD) in meters from (*47*). The purple circles identify the TPs on this record; C) Estimate of the CO_2 concentration in parts per million volume (ppmv) from (*48*). The Antarctica glaciation threshold at 750 ppmv and the NH glaciation threshold at 280 ppmv lines respectively are from (*85*).

Fig. 4. **Quasi-Potential topography of the climate system in the CENOGRID benthic $\delta^{18}O$ and $\delta^{13}C$. space.** Probability Density plot with the Tipping points ordered by priority according to the recurrence analysis for $\delta^{18}O$; the approximate timing is also indicated (rounded to 1 My). 50 Kyr before and after each TP (indicated by the white diamond) is also plotted. Darker blue hues indicate that we are going to the more distant past. Each dot corresponds to 2 Kyr. One point every 50 Ky from the time series is also added; darker magenta indicate more distant past, showing the direction of evolution of the climate.

Fig. 5. **Evolution of the Earth Climate history among 2 different tipping landscapes and proposal for a potential third one.** The first landscape in light red, corresponds to the Hot-Warm House time interval. The second landscape in light blue corresponds to the Cold-Ice house time interval. The third landscape, in light green, corresponds to the potential new one represented by the Anthropocene time interval. The different abrupt transitions identified in

the present study are reported as TP or CT to differentiate the major tipping points from the critical transitions characterizing transitions of lighter significance in the climate history. Various plate tectonic and ice sheet events are indicated and supported by maps of plate movements and North and South Hemisphere ice sheets. The Antarctica maps are from (*86*), Northern Hemisphere ice sheet maps are from (*87*). The paleogeographic maps have been generated using the Ocean Drilling Stratigraphic Network (ODSN) plate tectonic reconstruction service: < https://www.odsn.de/odsn/services/paleomap/paleomap.html>. The red arrows on the tectonic maps indicate the key events at the identified abrupt transition.

Supplementary Materials

Please use the *Science Advances* template to format your Supplementary Materials.